

Research Article

# The Structural Behavior of Lightweight Self-Compacting Concrete Slabs Using Different Types of Reinforcement

Fatma Mohamed Eid<sup>1,\*</sup> , Islam Ali Mahmoud<sup>2</sup> 

<sup>1</sup>Department of Civil Engineering, Menoufia University, Shibeh Elkom, Egypt

<sup>2</sup>Department of Civil Engineering, Delta Higher Institute for Engineering and Technology, Mansoura, Egypt

## Abstract

The purpose of this study is to examine how the type of reinforcement used in self-compacting concrete (SCC) and lightweight self-compacting concrete (LWSCC) affects their structural behavior. There were three forms of reinforcement used: wire mesh, glass fiber-reinforced rebars, and regular steel rebars. To evaluate the mechanical characteristics of reinforced concrete slabs with various types of reinforcement, extensive experiments were carried out. The tensile strength, stiffness, and crack resistance of the concrete were studied in each case. The finite element program Abaqus was utilized in addition to the experimental investigations to create the numerical simulation of the test. The experimental results revealed that the reinforcement type significantly affects the structural behavior of SCC and LWSCC slabs. Conventional steel rebars provided high tensile strength and excellent crack resistance, while glass fiber-reinforced rebars contributed to enhanced flexibility and reduced overall weight of the concrete. On the other hand, the wire mesh exhibited average mechanical and structural properties. These findings emphasize the importance of selecting the appropriate reinforcement type based on specific applications and desired performance requirements. This research provides valuable guidance for architects and civil engineers in choosing optimal reinforcement for SCC and LWSCC. Furthermore, it can contribute to the advancement of techniques and potential improvements in these materials to achieve better performance and enhance sustainability in infrastructure and building construction. From the practical results, it was found that in the case of using lightweight self-compacting concrete and self-compacting concrete, it is preferable to reinforce it with ordinary reinforcement steel, as it gives the best results in terms of maximum load capacity at failure. Although the use of steel reinforcement in self-compacting concrete also gives the best results, but from the laboratory results it is possible to improve the performance of self-compacting concrete by reinforcing it with GFRP or welded wire mesh.

## Keywords

Self-compacting Concrete, Lightweight Self-Compacting Slabs, Finite Element Analysis, ABAQUS

## 1. Introduction

Concrete is often the most widely utilized building material worldwide because of its accessibility, durability, affordability, and sustainability. Additionally, concrete has been regarded as the most widely used building material because of its ex-

\*Corresponding author: fatma\_elzahraa2002@yahoo.com (Fatma Mohamed Eid)

**Received:** 14 August 2024; **Accepted:** 7 September 2024; **Published:** 26 September 2024



Copyright: © The Author(s), 2024. Published by Science Publishing Group. This is an **Open Access** article, distributed under the terms of the Creative Commons Attribution 4.0 License (<http://creativecommons.org/licenses/by/4.0/>), which permits unrestricted use, distribution and reproduction in any medium, provided the original work is properly cited.

tremely low cost. Due to its superior compatibility and filling capacity over regularly vibrated concrete (NVC), self-compacting concrete (SCC) has drawn a lot of attention from the civil engineering community in recent decades. For a considerable amount of time, SCC has shown to be a revolutionary invention that improves flow and workability and distributes under the weight without requiring mechanical compaction. Its exceptional flow ability makes it ideal for intricate and crowded structures, enabling faster production with less effort and noise. Scholarly researches indicate that, in comparison to NVC mixes, SCC mixes exhibit statistically significant improvements in strength and durability [1, 2]. Sustainability is becoming a major concern for researchers these days, one of the main users of raw materials has historically been thought to be the building sector, and overuse of natural resources contributes to pollution and environmental degradation, the output of garbage from construction and demolition has expanded recently along with developments in the construction sector, to protect natural resources, several studies have been conducted on the use of recycled aggregate made from industrial and demolition debris [4]. The use of LWA (Light Weight Aggregate) in LWSCC (Light Weight Self Compact Concrete) can significantly affect compressive strength because its strength is substantially lower than that of ordinary aggregates. Various LWA types are employed in the manufacturing of LWSCC, and because of variations in their physical characteristics, the density and strength of LWSCC can vary [3, 5]. Concrete made with low-strength LWA may have low compressive strength because of the variance in LWAs' properties at comparable mixing percentages. The authors compared the compressive strength of scoria- and LECA-based LWSCC made at identical mixing compositions, finding that the former had a lower compressive strength than the latter [5]. Found a comparable inconsistency in compressive strength with essentially the same mixing composition. These investigations show that the compressive strength of concrete may be significantly reduced by the use of highly porous LWAs such as pumice, expanded glass, polystyrene, and LECA. A larger percentage of LWA in the concrete mix was shown to cause a greater loss in compressive strength [6]. Examine the effects of micro-silica (MS) and sand fineness modulus (FM) on the characteristics of self-compacting concrete (SCC) and self-compacting lightweight concrete (SCLC). The findings demonstrated that raising the sand FM enhanced SCC and SCLC's fresh and toughened qualities. Lightweight aggregates, such as Lightweight Expanded Clay Aggregate (LECA), can be added to the concrete mixture to help with the weight reduction problem [7, 8]. Lightweight concrete (LWC) can be created by substituting lighter coarse particles for traditional ones, with a unit weight of less than  $2000 \text{ kg/m}^3$  [9]. The flexural behavior of self-compaction, self-curing concrete (SCSCC) beams by utilizing fly ash aggregates (FAA) and lightweight expanded clay aggregates (LECA) was studied, the test findings show that the 15% substitution of fine aggregate by LECA/FAA produced higher

moment carrying capacity and ductility ratio, as well as load-deflection behavior and beam ductility ratio [10]. The effects of light-expanded clay aggregate content and maximum size was on the fresh, strength, and durability characteristics of self-compacting lightweight concrete reinforced with micro steel fibers were studied the findings showed that when maximum size of aggregate ( $d_{\max}$ ) increased, less super plasticizer was needed to maintain the slump flow at 700–750 mm. The best compressive and flexural strengths were obtained at a  $d_{\max}$  of 10 mm. As the  $d_{\max}$ , LECA concentration, and volume fraction of micro steel fibers ( $V_f$ ) increased, the water sorptivity generally increased as well. On the other hand, drying shrinkage often decreased as ( $d_{\max}$  and  $V_f$ ) increased [11]. The glass fiber content and LECA affected the structural and physical characteristics of lightweight concrete according to the study, increasing the amount of glass fibers did not always lead to better mechanical qualities. Controlling the ratio of glass fibers to LECA can result in more perfect characteristics. It is strongly recommended to narrow down the glass fiber content range to 2% and combine it with an LECA content of 75% and 85% after conducting experiments to achieve the optimal behavior of glass fiber-reinforced LECA concrete [12].

## 2. Experimental Program

### 2.1. Materials

#### 2.1.1. Cement

The Suez cement factory produces Ordinary Portland cement, which was the type of cement utilized. According to the Egyptian Standard Specification (E.S.S. 4657-1/2009), its physical and chemical properties were met [14].

#### 2.1.2. Fine Aggregate

Fine aggregates were made from natural siliceous sand from the Menoufia government's El-Khatatba. The Egyptian Code (E.C.P. 203/2007) 10 and (E.S.S. 1109/2008) [15] are satisfied by its features. It had a specific gravity of  $2.6 \text{ t/m}^3$  and a modulus of fineness of 2.7, meaning it was almost pure and devoid of contaminants.

#### 2.1.3. LECA

The lightweight aggregate used in this study, locally produced from expanded clay (LECA), and had a maximum nominal size of 15 mm. Before mixing into concrete, the dry LECA was soaked in water for 48 hours to ensure all internal voids were filled.

#### 2.1.4. Water

The test specimens are mixed and cured in pure drinking fresh water devoid of contaminants.

### 2.1.5. Silica Fume

The Sika Group developed silica fume, which was used to partially replace cement in mortar mixes to boost their permeability and strength. The powder form was given in a light grey color. When combined with mortar, it yields a black slurry. Commercial purchases of it are made under the ASTM (C1240-03) compliant ACC Micro Silica Grade [16].

### 2.1.6. Super Plasticizer

High range water reducer, or HRWR, was employed with Super Plasticizer. It was applied to increase the mix's workability. The admixture that was employed complies with ASTM C494-92 (type F) criteria and was manufactured by Sika Group under the trade name SIKAMENT NN [17]. Two percent of the cement weight was HRWR.

### 2.1.7. Polypropylene Fibers

It was accessible in the markets of Egypt. Based on the manufacturer's recommendations, 900 gm/m<sup>3</sup> was selected as

the addition. The Polypropylene Fibers PP 300-e3 producing company's technical specs and mechanical qualities are included in Table 1. Figure 1a describe the shape of the (PP) fibers.

### 2.1.8. Expanded Wire Mesh

Ferrocement plates were reinforced with expanded wire mesh. It satisfies the Egyptian Standard Specification (E.S.S. 262/2011) in terms of both chemical and physical properties [18]. Table 2 displays the mechanical characteristics and technical specifications of the welded metal mesh, along with its shape as seen in Figure 1b.

### 2.1.9. Reinforcing Steel

The standard mild steel bars were made by Ezz Al Dekhila Steel in Alexandria. The Egyptian Standard Specification (E.S.S. 262/2011) is satisfied by its chemical and physical properties [19]. The ferrocement plates were reinforced with steel bars, which had nominal diameters of 6 mm and yield stresses and tensile strengths of 240 MPa and 350 MPa, respectively.

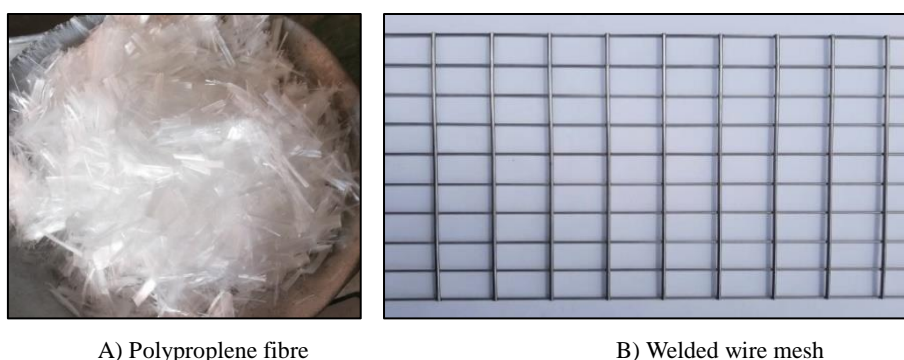


Figure 1. The used materials.

Table 1. The 300-e3 polypropylene fibers' mechanical and physical characteristics.

Fiber Length	Type / Shape	Absorption	Specific Gravity	Electrical Conductivity	Acid And Salt Resistance	Melt Point	Ignition Point	Thermal Conductivity	E-Modulus
Graded	Fibrillated	Nil	0.91	Low	High	162 °C	593 °C	Low	3.5 GPa

Table 2. Expanded wire mesh technical details and mechanical characteristics.

Sheet size	Weight	Diamond size	Dimensions of strand	Proof Stress	Proof Strain	Ultimate Strength	Ultimate Strain
1 × 10 m	1.3 Kg/m <sup>2</sup>	16 × 31 mm	1.25 × 1.5 mm	199 N/m m <sup>2</sup>	9.7 × 10 <sup>-3</sup>	320 N/m m <sup>2</sup>	59.2 × 10 <sup>-3</sup>

By knowing the percentage of the components of the concrete mixture and the basis of the mixtures, the components of two

groups (1 and 2) of the concrete mixture were calculated based on the volume of a cubic meter. Light-weight self-compacting concrete (LWSCC) was used in group (1) using lightweight expanded clay aggregate (LECA), While group (2) utilized self-compacting concrete (SCC). Tables 3 and 4 specifies the amounts of mixture needed to make one cubic meter of LWSCC and SCC material respectively.

**Table 3.** Mix quantities to produce  $1m^3$  of LWSCC in group (1).

Cement (kg)	Silica Fume (kg)	Fly ash (kg)	Sand (kg)	Water (kg)	LECA (kg)	Vescocrete (kg)
382	81	76	900	153	13.65	5.1

**Table 4.** Mix quantities to produce  $1m^3$  of SCC in group (2).

Cement (kg)	Silica Fume (kg)	Dolomite (kg)	Sand (kg)	Water (kg)	Vescocrete (kg)
500	50	956	637	210	4

## 2.2. Test Specimens

Ten concrete slabs were cast for this study with dimensions (1000 × 500 × 50) mm to research many variables that may impact structural behavior as shown in Figure 2. The first five slabs in the first group were cast using lightweight self-compact concrete (LWSCC) with the sample names from S1 to S5. The five slabs in the second group were poured with self-compact concrete (SCC) with the sample names from S6 to S10. The first sample of each group is the control slab that was poured without any glass fibers and reinforcement steel. To study the effect of the proportion and type of reinforcement steel on the mechanical properties of the slab, four models of each type of concrete were made with different shapes and proportions of steel. Whereas slabs S2 and S7 were reinforced with 6Φ10 of GFRP for each meter in two directions of the

slab as viewed in Table [5]. In contrast, as can be seen in Table [5], slabs S3 and S8 were strengthened with steel reinforcement 6 by 10 for every meter in both directions of the slab. On the other hand, as can be seen in Table [5], slabs S4 and S9 were strengthened with GFRP reinforcement 3Φ10 and expanded steel mesh. Finally, the S5 and S10 slabs were reinforced with welded wire mesh and glass fiber was placed in the concrete during casting. Ordinary rebar produced by the Ezz El Dekheila Factory in Sadat City was used, conforming to Egyptian standard specifications (M.S.C. 262), and bars with a diameter of 10 mm were used. The reinforcement's yield strength and Young's modulus were 368 GPa and 210 MPa, respectively. Glass fiber bars were used and a tensile test was conducted. The results of the tensile test showed that the maximum strength of the GFRP is 493.3 GPa at 0.0257 elongation at break.

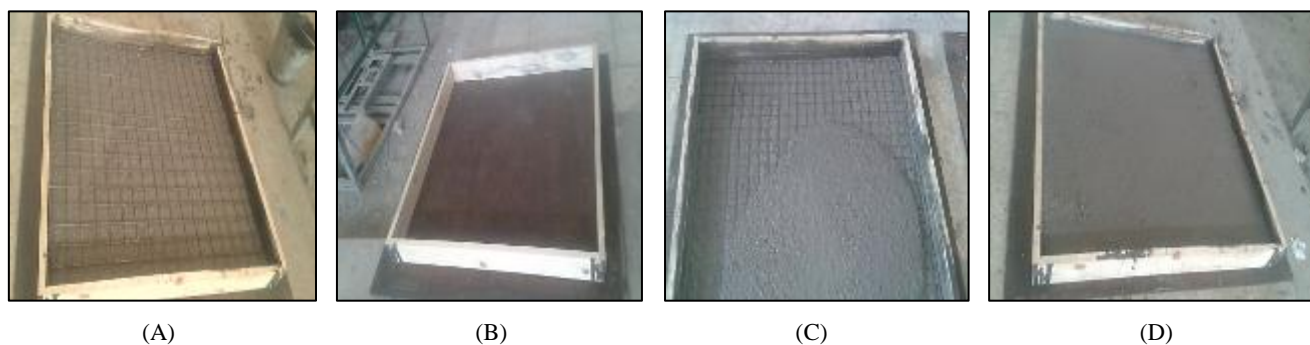


**Figure 2.** Casting of specimens.

**Table 5.** Details of tested slabs.

Group	Slab ID	Type of concrete Mix	Type of reinforcement	HZ. Section
1	S1	LWSCC	None	
	S2	LWSCC	GFRP Bars 6 Ø 10 in two direction	
	S3	LWSCC	Steel Bars 6 Ø 10 in two direction	
	S4	LWSCC	GFRP Bars 3Ø 10 in two directions + Steel mesh	
	S5	LWSCC	Steel mesh + Glass fiber	
2	S6	SCC	None	
	S7	SCC	GFRP Bars 6 Ø 10 in two direction	
	S8	SCC	Steel Bars 6 Ø 10 in two direction	
	S9	SCC	GFRP Bars 3Ø 10 in two directions + Steel mesh	
	S10	SCC	Steel mesh + Glass fiber	

### 2.3. Test Setup

The specimens were put through testing in a 1000 kN machine as shown in Figure 3. Slabs were simply supported throughout 900 mm as shown in Figure 4. Two plates spaced 300 mm apart were used to spread the load. The symmetry between the two loads and the slab's centerline. 300 millimeters are separating the two loading plates. The edge dimensions of the nearest support and the load plate are 300 mm. For every 0.5 kN increment of load, the deflection at the centerline was measured using a linear variable differential transformer (LVDT) positioned at the center. The load value was recorded at the first crack that occurred for each sample of the slabs studied.



**Figure 3.** The machine that tested the samples.

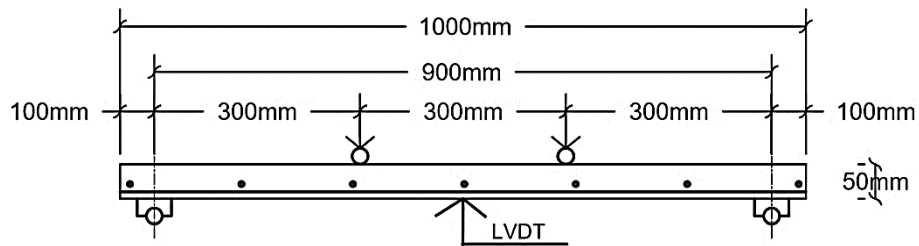


Figure 4. Testing setup details.

### 3. Experimental Results and Discussion

Immediately after the mixing, the value of slump flow, and J-ring were determined [14]. The slump flow test was used to evaluate the free deformability and flow ability of (LWSCC), and (SCC) in the absence of obstruction according to EF-NARC [20].

The compressive strength of light weight self-compacted concrete at 28 days age was determined according to ASTM C39-86 [21]. Table 6 shows the compressive strength of the investigated mixes.

#### 3.1. Initial Crack Load and Ultimate Load

Every slab specimen was examined until the first break appeared, at which point the associated load was recorded. Table 6 presents an overview of the significant experimental outcomes for the examined specimens. It was observed that when using reinforced steel lightweight self-compact concrete (LWSCC), it gives the best values in terms of ultimate load

and cracking load. It was also noted from the practical results that it is better to use reinforcing steel in self-compacted concrete (SCC). The maximum load capacity increased from 770 to 1010 kN when using SCC instead of lightweight LWSCC, with an increase of 23.8% as shown in Figure 5 and Figure 6.

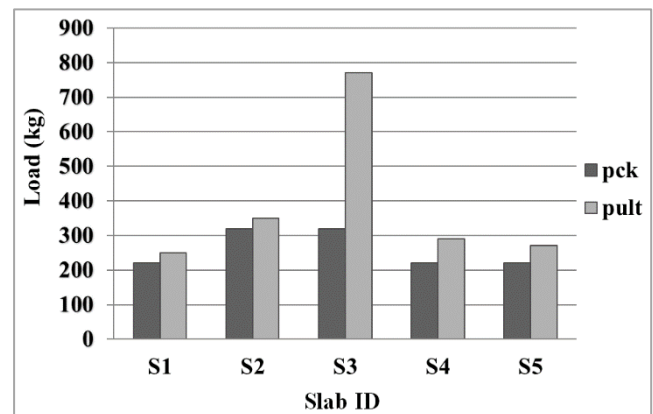


Figure 5. The ultimate load and cracking load for group (1).

Table 6. Experimental results.

Group	Slab ID	Fiber content (PP) %	Concrete cube compressive strength (MPa)	Concrete cube tensile strength (MPa)	Initial cracking load, P <sub>CR</sub> (kN)	Ultimate load, P <sub>ULT</sub> (kN)	Maximum Mid-span Deflection (mm)
1	S1	-	25	2.4	2.20	2.50	7
	S2	-	25	2.4	3.20	3.50	3.63
	S3	-	25	2.4	3.20	7.70	21.52
	S4	-	25	2.4	2.20	2.90	15.51
	S5	1	25	2.65	2.20	2.70	0.68
2	S6	-	50	5.2	2.70	3.00	0.59
	S7	-	50	5.2	3.20	6.20	0.74
	S8	-	50	5.2	3.70	10.10	0.86
	S9	-	50	5.2	3.70	5.40	0.55
	S10	1	50	5.75	3.50	5.10	1.42

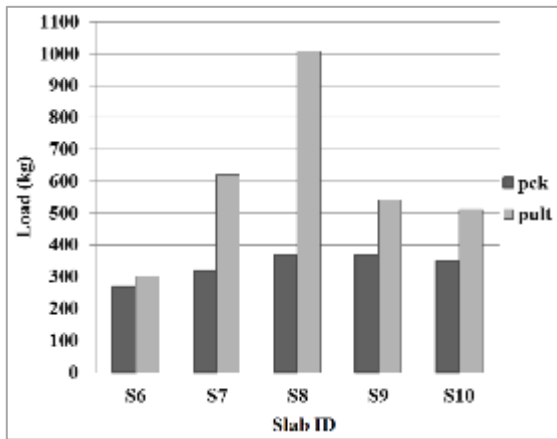


Figure 6. The ultimate load and cracking load for group (2).

### 3.2. Load-Deflection Response

Figures 7 and 8 show the experimental load to mid-span deflection curves. The charts show the deflection value determined by the LVDT installed in the middle of the slab.

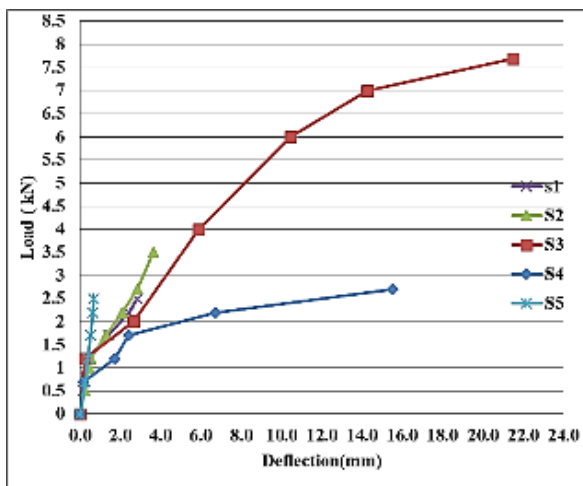


Figure 7. Load & deflection curve for group (1).

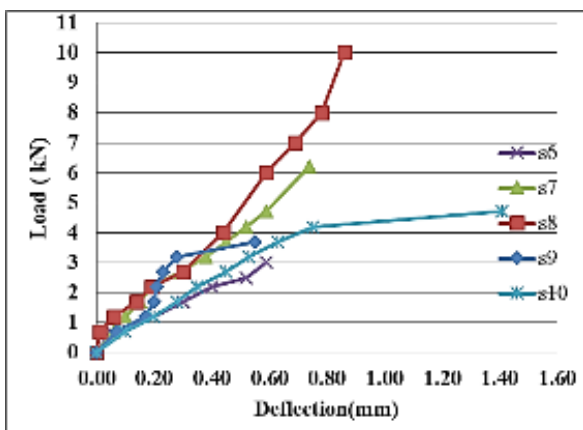
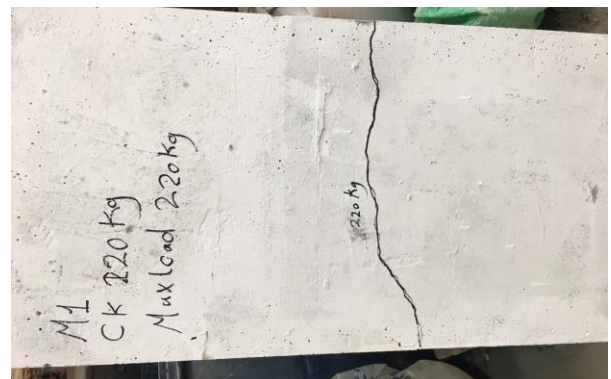


Figure 8. Load & deflection curve for group (2).

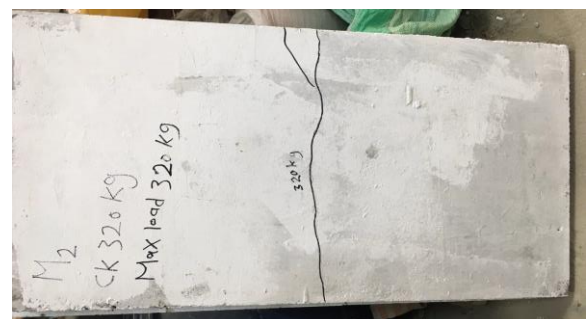
### 3.3. Mode of Failure

The flexure of the specimens was experimentally examined using four-point loading tests. For every slab, flexure failure was identified as the kind of failure. When the load was increased, the slabs began to break in the high bending moment zone and subsequently spread vertically. When the load was increased, the slabs began to break in the high bending moment zone and subsequently spread vertically. Group B's failure mode and crack pattern are depicted in Figures 10a–e.

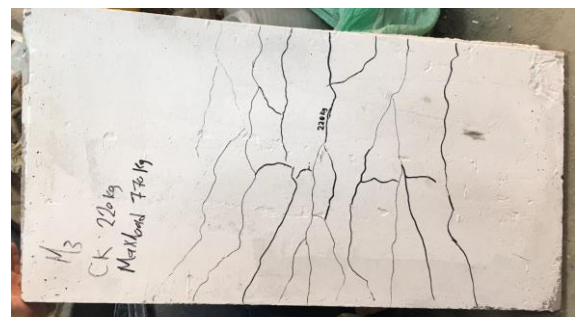
It is evident that the same failure mode that was shown for Group A was also displayed.



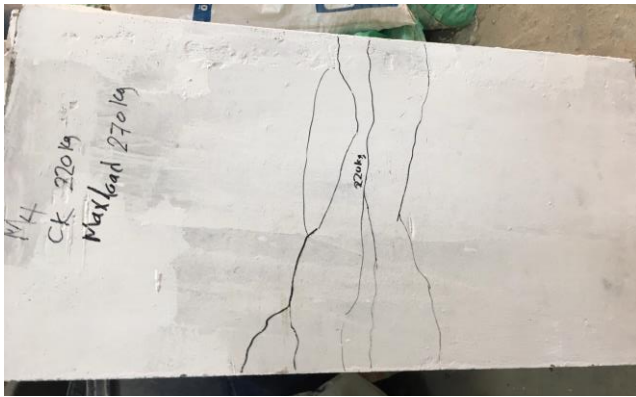
S1



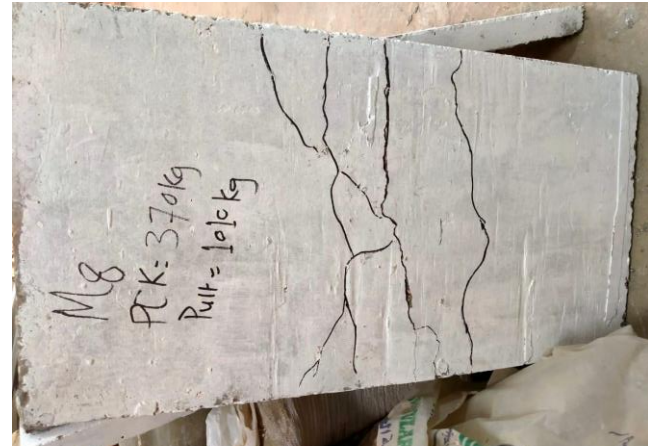
S2



S3



S4



S8



S5



S9

**Figure 9.** Cracks pattern of Group (1).



S6



S10

**Figure 10.** Cracks pattern of Group (2).



S7

#### 4. Non-Linear Finite Elements Analysis

To simulate the tested slabs, non-linear finite elements analysis was performed. Software package, ABAQUS [13], was the method used at the time to carry out the analysis. The load-deflection curve is a crucial tool for examining the slab's mechanical behavior. It contains response parameters like

maximum deflection and ultimate loads. Therefore, it is thought that an effective way to validate the non-linear model is to compare the load-deflection curves that are taken from the analytical results with the curves from the experiments. Specialized skills are necessary while working with reinforced concrete. This means that a finite element model needs to be developed in order to predict the elastic and plastic behavior of concrete under tension and compression. Information characterizes the LWSCC stress-strain curve in tension and compression, as shown in Table 7. Information characterizes the SCC stress-strain curve during compression and tension, as shown in Table 8.

**Table 7.** Data defines the LWSCC in compression and tension.

Data define for compression		
Stress $\sigma_c$ (N/m <sup>2</sup> )	Plastic strain ( $\epsilon_{pl}$ )	Damage parameter (dc)
17.80143	0	0
18.93227	4.71233E-06	0
20.02894	1.23035E-05	0
21.07689	2.40005E-05	0
22.94663	6.64513E-05	0
23.71678	0.000101556	0
24.76896	0.000212896	0
25	0.000293428	0
24.64192	0.000523601	0.014323
22.11118	0.001036848	0.115553
21.08705	0.001203145	0.156518
19.36693	0.001468087	0.225323
14.69332	0.002161899	0.412267
13.1885	0.002388699	0.47246
10.45341	0.002819166	0.581864

Data define for tension		
Stress $\sigma_t$ (N/m <sup>2</sup> )	Plastic strain ( $\epsilon_{pl}$ )	Damage parameter (dt)
2.4	0	0
0.95928	0.000319	0.52036
0.59616	0.00065	0.70192
0.481493	0.000859	0.759253
0.440247	0.000963	0.779877

**Table 8.** Data defines the SCC in compression and tension.

Data define for compression		
Stress $\sigma_c$ (N/m <sup>2</sup> )	Plastic strain ( $\epsilon_{pl}$ )	Damage parameter (dc)
25.26769	0	0
27.36442	4.22714E-07	0
29.454	1.18556E-06	0
35.6296	7.89667E-06	0
39.57773	2.03944E-05	0
43.23969	4.64823E-05	0
44.89921	6.7669E-05	0
48.75114	0.000184735	0
49.92968	0.000328764	0
50	0.000425425	0
49.58916	0.000544936	0.008217
45.8932	0.001020463	0.082136
41.56299	0.001426111	0.16874
39.01428	0.001647153	0.219714
30.76413	0.002338965	0.384717
25.44296	0.002791676	0.491141

Data define for tension		
Stress $\sigma_t$ (N/m <sup>2</sup> )	Plastic strain ( $\epsilon_{pl}$ )	Damage parameter (dt)
5.2	0	0
3.904439	0.000215	0.34926
2.766184	0.000469	0.538969
2.166123	0.000697	0.638979
1.791883	0.000915	0.701353

*Finite Element Analysis and Mesh*

Table 9 lists the types of finite elements that were utilized in the finite element formulation.

**Table 9.** Finite element types that are applied in numerical simulation.

Description	Type	Part
8-node linear brick with hourglass control	C3D8R	Concrete Slab
2-node, three-dimensional	T3D2	Longitudinal Steel

Description	Type	Part
truss element		
2-node, three-dimensional truss element	T3D2	Expanded Steel Mesh

As seen in Figure 11, a fine mesh with an element size of 10 mm was incorporated into the model for improved finite element accuracy after a convergence analysis. The whole model geometry is shown in Figure 12.

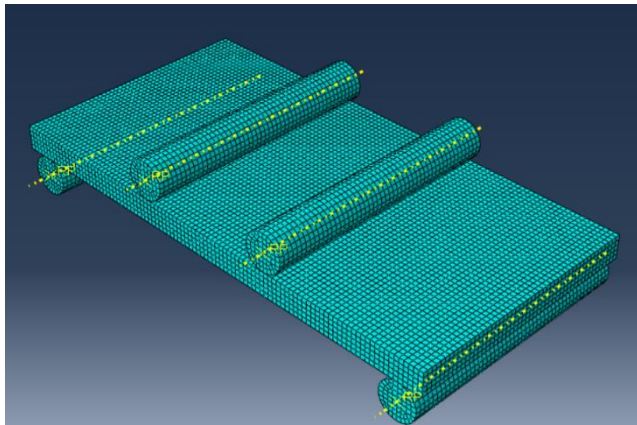


Figure 11. Mesh of finite elements.

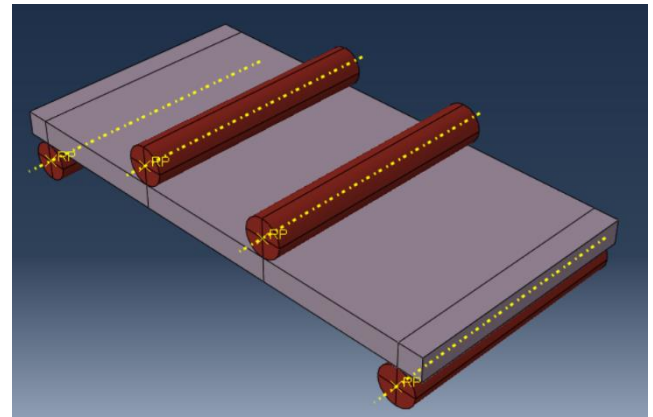


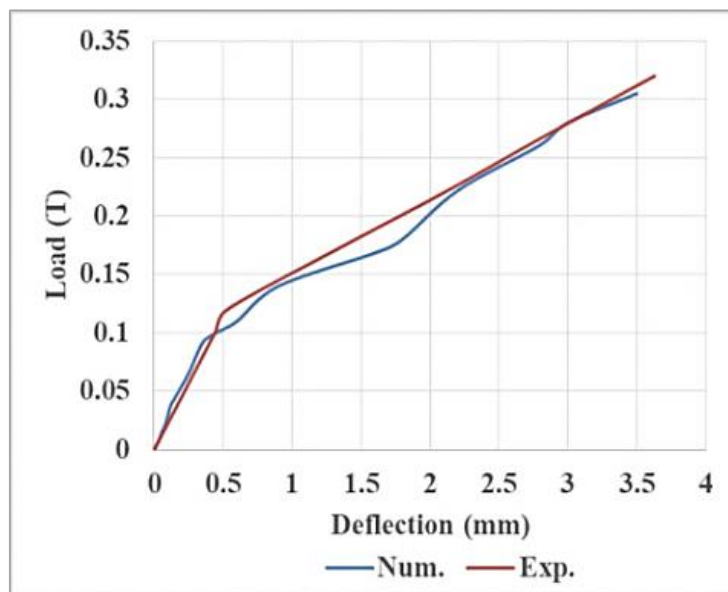
Figure 12. Model's geometry.

## 5. Verification of Results and Discussion

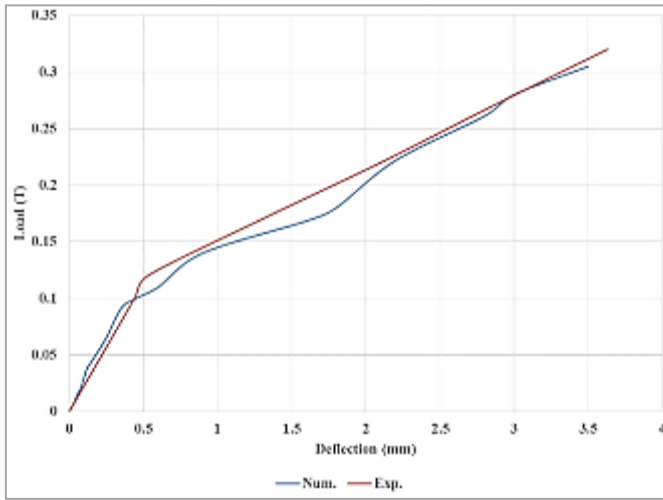
An excellent agreement was found between the load-deflection responses of the numerical model and the experimental results. Figures 13 to 14 compare the load-deflection graphs from ABAQUS with the experimental results for each of the 10 slabs.

### 5.1. Load Deflection Curves

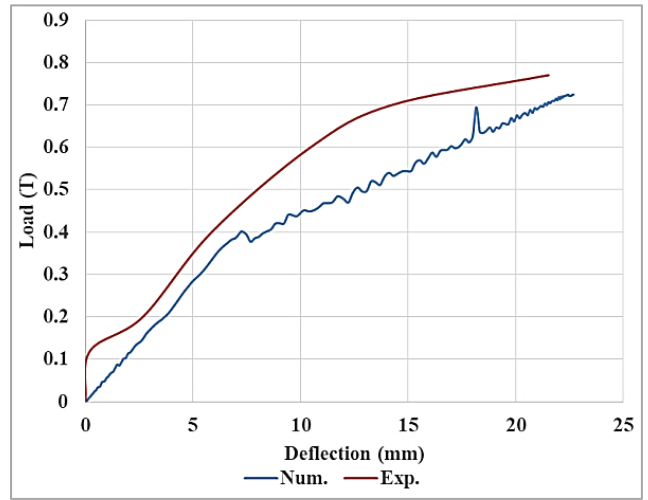
Figures 13 to 14 compare the load-deflection graphs from ABAQUS [13] with the experimental results for each of the 10 slabs. The test result curve varied slightly. This is because, although perfect bonding between the concrete and the steel reinforcement is assumed in finite element analysis, the slab that was subjected to experimental testing would not support this assumption.



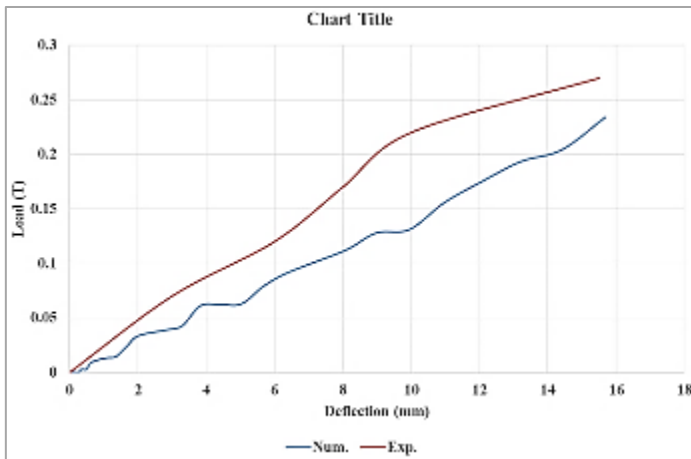
S1's load-related deflection



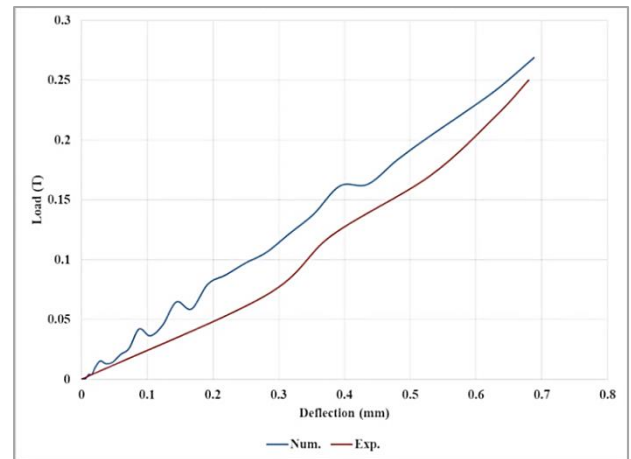
S2's load-related deflection



S3's load-related deflection

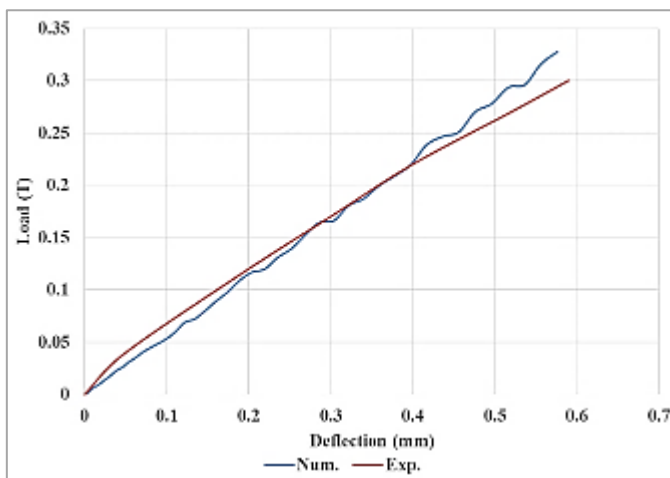


S4's load-related deflection

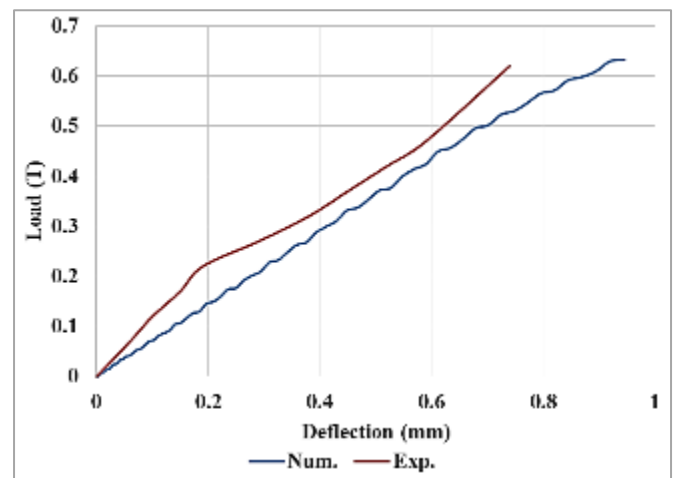


S5's load-related deflection

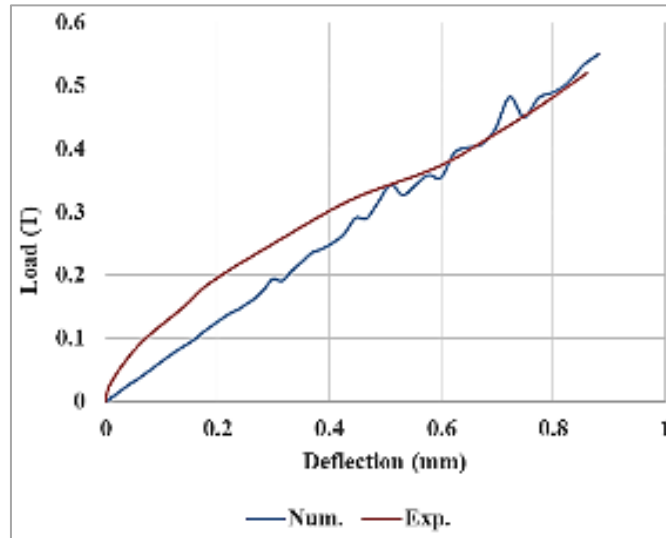
Figure 13. Comparisons of group 1's experimental and numerical results.



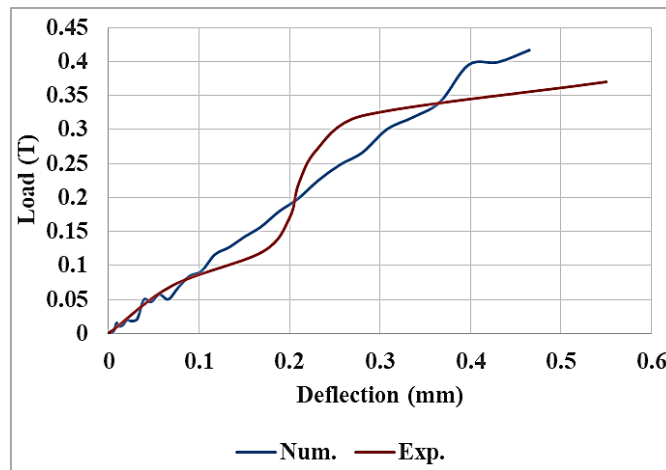
S6's load-related deflection.



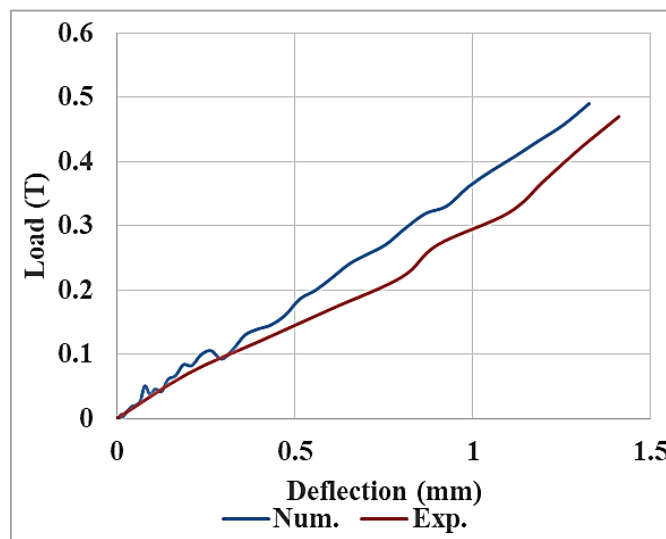
S7's load-related deflection



S8's load-related deflection



S9's load-related deflection



S10's load-related deflection

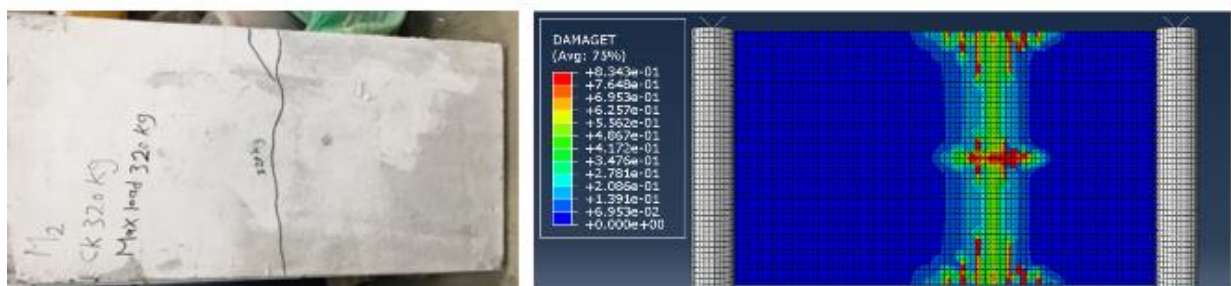
Figure 14. Comparisons of group 2's experimental and numerical results.

## 5.2. Mode of Failure

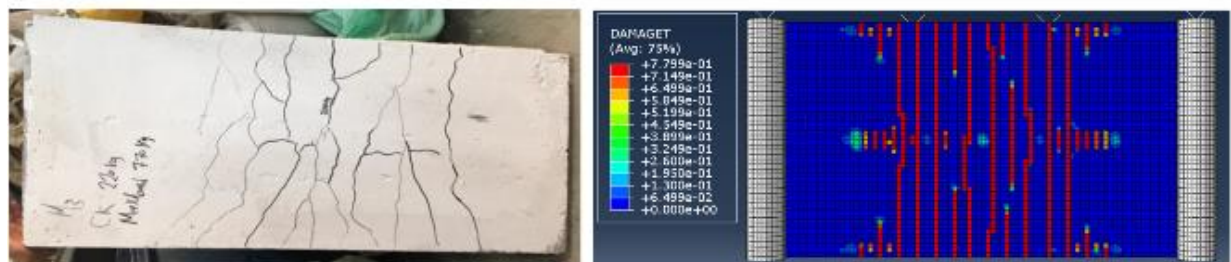
Good agreement was found when comparisons were made between the experimental failure mode and the slab's finite element analysis. as shown in Figures 15, 16.



Comparisons of slab S1 failure mechanisms using numerical and experimental methods



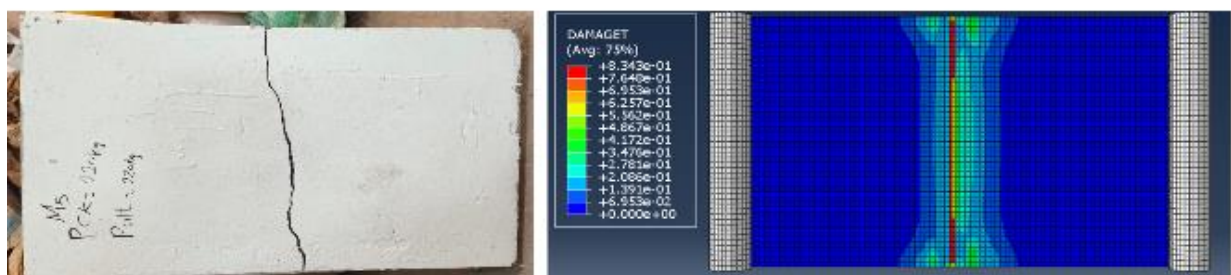
Comparisons of slab S2 failure mechanisms using numerical and experimental methods



Comparisons of slab S3 failure mechanisms using numerical and experimental methods

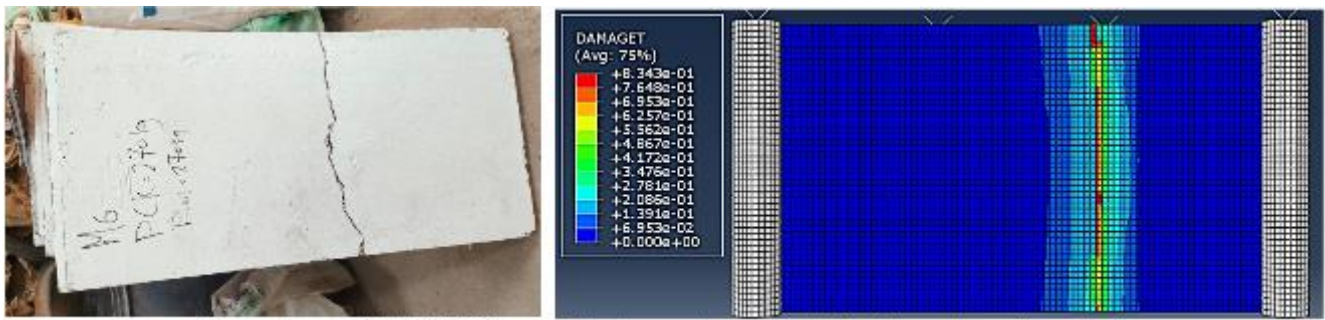


Comparisons of slab S4 failure mechanisms using numerical and experimental methods

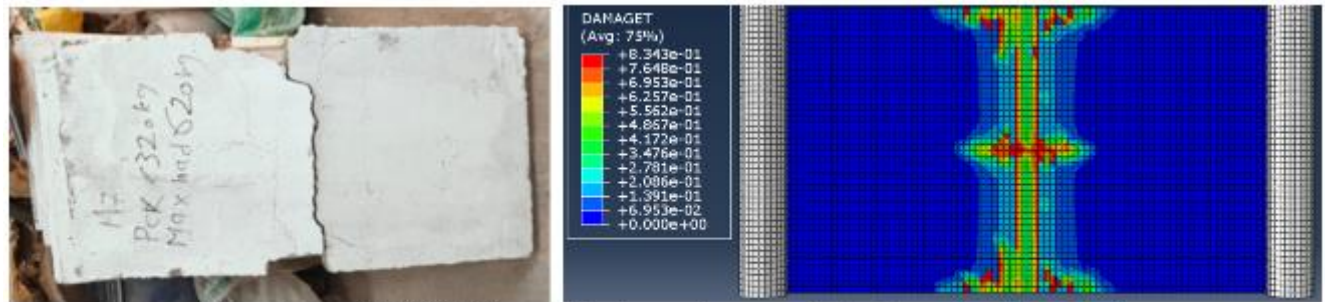


Comparisons of slab S5 failure mechanisms using numerical and experimental methods

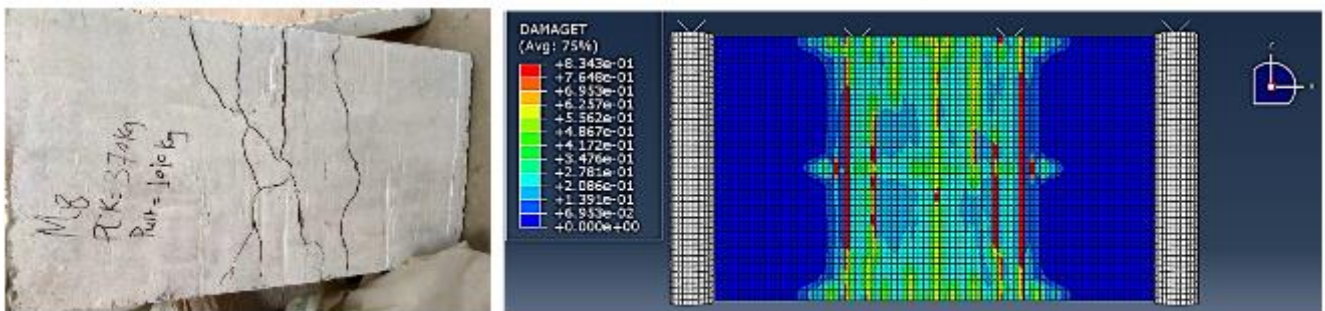
Figure 15. Comparison of slab failure mechanisms in group (1) using numerical and experimental methods.



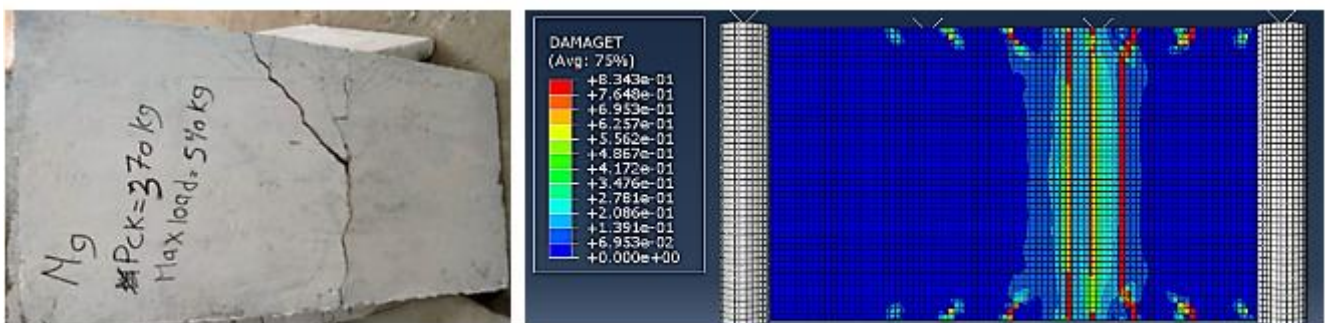
Comparisons of slab S6 failure mechanisms using numerical and experimental methods



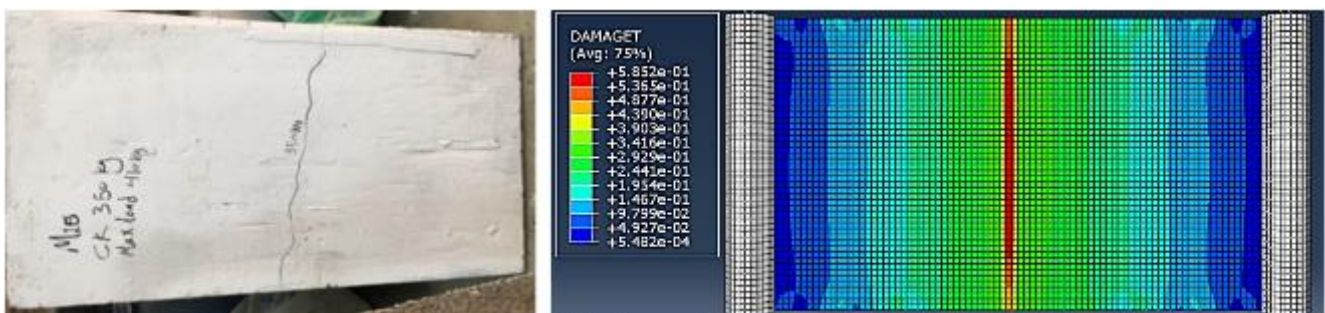
Comparisons of slab S7 failure mechanisms using numerical and experimental methods



Comparisons of slab S8 failure mechanisms using numerical and experimental methods



Comparisons of slab S9 failure mechanisms using numerical and experimental methods



Comparisons of slab S5 failure mechanisms using numerical and experimental methods

Figure 16. Comparison of slab failure mechanisms in group (2) using numerical and experimental methods.

## 6. Conclusion

This research aims to investigate the impact of changing the reinforcement type on the structural behavior of self-compacting concrete (SCC) and lightweight self-compacting concrete (LWSCC). Three different types of reinforcement were utilized, including conventional steel rebar, glass fiber-reinforced rebar, and wire mesh. Extensive tests were carried out to evaluate the mechanical characteristics of reinforced concrete slabs featuring every kind of reinforcement:

1. From the practical results, it was found that in the case of using lightweight self-compacting concrete and self-compacting concrete, it is preferable to reinforce it with ordinary reinforcement steel, as it gives the best results in terms of maximum load capacity at failure.
2. Although the use of steel reinforcement in self-compacting concrete also gives the best results, but from the laboratory results it is possible to improve the performance of self-compacting concrete by reinforcing it with GFRP rebar or welded wire mesh.
3. When using ordinary reinforcement steel, it also gives ductile collapse, unlike using GFRP.
4. The load capacity of S3 slab was observed increased by 208% when adding ordinary steel reinforcement. Where the load capacity increased from 2.5 kN of S1 slab to 7.7 kN of S3 slab.
5. When reinforcing the slab cast with lightweight self-compacting concrete with GFRP steel, the maximum load capacity has been increased by 56%.
6. When the slab cast with lightweight self-compacting concrete is reinforced with welded wire mesh, the maximum load is slightly increased.
7. The load capacity of S8 slab was observed increased by 236.67% when adding ordinary steel reinforcement. Where the load capacity increased from 3 kN of S1 slab to 10.10 kN of S3 slab.
8. When reinforcing the slab cast with self-compacting concrete with GFRP steel, the maximum load capacity has been increased by 106.6%. From this result, the use of GFRP rebar in self-compacting concrete improves its load capacity.
9. When reinforcing the slab cast with self-compacting concrete with welded wire mesh, the maximum load capacity has been increased by 70.0%. From this result, the use of welded wire mesh in self-compacting concrete improves its load capacity.
10. The shape of the collapse showed a strong agreement when the experimental and numerical data were compared.
11. An excellent agreement was found between the load-deflection responses of the numerical model and the experimental results.

## Abbreviations

SCC	Self-Compacting Concrete
LWSCC	Lightweight Self-Compacting Concrete
GFRP	Glass Fiber-Reinforced Rebars
NVC	Regularly Vibrated Concrete
LECA	Lightweight Expanded Clay Aggregate
FAA	Fly Ash Aggregates
$d_{max}$	Maximum Size of Aggregate
$V_f$	Volume Fraction of Micro Steel Fibers

## Author Contributions

**Fatma Mohamed Eid:** Conceptualization, Formal Analysis, Funding acquisition, Methodology, Project administration, Resources, Supervision, Writing – original draft, Writing – review & editing

**Islam Ali Mahmoud:** Formal Analysis, Investigation, Software, Validation, Writing – original draft, Writing – review & editing

## Conflicts of Interest

The authors declare no conflicts of interest.

## References

- [1] Şenol, A., Karakurt, C., (2024). “High-strength self-compacting concrete produced with recycled clay brick powders: Rheological, mechanical and microstructural properties”. *Journal of Building Engineering*. <https://doi.org/10.1016/j.jobbe.2024.109175>
- [2] H. Zhang, B. Zhang, L. Tang, W. Zeng, (2023). “Analysis of two processing techniques applied on powders from recycling of clay bricks and concrete, in terms of efficiency, energy consumption, and cost, Construction and Building Material”, <https://doi.org/10.1016/J.CONBUILDMAT.2023.131517>
- [3] Aslani, F., Ma, G., (2018). “Normal and High-Strength Lightweight Self-Compacting Concrete Incorporating Perlite, Scoria, and Polystyrene Aggregates at Elevated Temperatures”. *Journal of Materials and Civil Engineering* 30, 04018328, [https://doi.org/10.1061/\(asce\)mt.1943-5533.0002538](https://doi.org/10.1061/(asce)mt.1943-5533.0002538)
- [4] Yashar, M., Behzad, V., (2021). “Effect of pre-coating lightweight aggregates on the self-compacting concrete”. <https://doi.org/10.1002/suco.202000744>
- [5] Yim Wan, D. S. L., Aslani, F., Ma, G., (2018). “Lightweight Self-Compacting Concrete Incorporating Perlite, Scoria, and Polystyrene Aggregates”. *Journal of Materials and Civil Engineering*, [https://doi.org/10.1061/\(asce\)mt.1943-5533.0002350](https://doi.org/10.1061/(asce)mt.1943-5533.0002350)

- [6] Dolatabad, Y. A., Kamgar, R., Jamali Tazangi, M. A., (2020). "Effects of perlite, leca, and scoria as lightweight aggregates on properties of fresh and hard self-Compacting concrete". *Journal of Advanced Concrete Technology*. 18, 633–647. <https://doi.org/10.3151/JACT.18.633>
- [7] Nikzad, Y., et al., (2024). "Effect of sand fineness modulus on SCC and SCLC properties" *Journal of Construction and Building Materials*. <https://doi.org/10.1016/j.conbuildmat.2024.135761>
- [8] S. Yang, et al., (2015), "Properties of self-compacting lightweight concrete containing recycled plastic particles", *Construction and Building Materials*, <https://doi.org/10.1016/j.conbuildmat.2015.03.038>
- [9] ASTM C 330/330M, (2014), *Standard Specification for Lightweight Aggregates for Structural Concrete*, ASTM International, West Conshohocken, PA, USA.
- [10] Gopi, R., Revathi, V., (2021). "Flexural behavior of self-compacting self-curing concrete with lightweight aggregates". *Journal of Materials Today: Proceedings*, <https://doi.org/10.1016/j.matpr.2020.11.019>
- [11] Nahhab, A. and Ketab, A., (2020). "Influence of content and maximum size of light expanded clay aggregate on the fresh, strength, and durability properties of self-compacting lightweight concrete reinforced with micro steel fibers". *Construction and Building Materials*, <https://doi.org/10.1016/j.conbuildmat.2019.117922>
- [12] Louay, A. et al., (2023). "Glass fiber for improved behavior of light expanded clay aggregate concrete beams: an experimental study". *Frattura ed Integrità Strutturale*, 1-16, <https://doi.org/10.3221/IGF-ESIS.65.01>
- [13] Simulia, "Abaqus 6.13 Abaqus/CAE User's Guide)," p. 1138, (2013).
- [14] E. S. S. 4756-1/2009, 2009, Egyptian Standard Specification for Ordinary Portland Cement, Egypt.
- [15] E. C. P. 203/2007, 2007, Egyptian Code of Practice: Design and Construction for Reinforced Concrete Structures, Research Centre for Houses Building and Physical Planning, Cairo, Egypt.
- [16] E. S. S. 1109/2008, 2008, Egyptian Standard Specification for Aggregates, Egypt.
- [17] Standard Specification for Use of Silica Fume as a Mineral Admixture in Hydraulic Cement Concrete, Mortar, and Grout ASTM (C1240).
- [18] Standard Specification for Chemical Admixtures for Concrete ASTM (C 494/C 494M – 99).
- [19] E. S. S. 262 /2011, 2011, Egyptian Standard Specification for Steel Bars, Egypt.
- [20] EFNARC, (2005), "The European Guidelines for Self Compacting Concrete", Specification, Production and Use The Self-Compacting Concrete European Project Group, pp. 63
- [21] ASTM C39, (2007), "Standard Test Method for Compressive Strength of Cylindrical Concrete Specimens", *Cement Standards and Concrete Standards*.